First Evidence for a Dose–Response Relationship in Patients Treated with ^{166}Ho Radioembolization: A Prospective Study

Remco Bastiaannet*, Caren van Roekel*, Maarten L.J. Smits, Sjoerd G. Elias, Wouter A.C. van Amsterdam, Dan Doan, Jip F. Prince, Rutger C.G. Bruijnen, Hugo W.A.M. de Jong, and Marnix G.E.H. Lam

University Medical Center Utrecht, Utrecht University, Utrecht, The Netherlands

^{166}Ho-microspheres have recently been approved for clinical use for hepatic radioembolization in the European Union. The aim of this study was to investigate the absorbed dose–response relationship and its association with overall survival for ^{166}Ho radioembolization in patients with liver metastases. **Methods:** Patients treated in the HEPAR I and II studies who underwent an ^{18}F-FDG PET/CT scan at baseline, a posttreatment ^{166}Ho SPECT/CT scan, and another ^{18}F-FDG PET/CT scan at the 3-mo follow-up were included for analysis. The posttreatment ^{166}Ho-microsphere activity distributions were estimated with quantitative SPECT/CT reconstructions using a quantitative Monte Carlo–based method. The response of each tumor was based on the change in total lesion glycolysis (TLG) between baseline and follow-up and was placed into 1 of 4 categories, according to the PERCIST criteria, ranging from complete response to progressive disease. Patient-level response was grouped according to the average change in TLG per patient. The absorbed dose–response relationship was assessed using a linear mixed model to account for correlation of tumors within patients. Median overall survival was compared between patients with and without a metabolic liver response, using a log-rank test. **Results:** Thirty-six patients with a total of 98 tumors were included. The relation between tumor-absorbed dose and both tumor-level and patient-level response was explored. At a tumor level, a significant difference in geometric mean absorbed dose was found between complete response (232 Gy; 95% confidence interval [CI], 178–303 Gy; $n = 32$) and stable disease (147 Gy; 95% CI, 113–191 Gy; $n = 28$) ($P = 0.01$) and between complete response and progressive disease (117 Gy; 95% CI, 87–159 Gy; $n = 21$) ($P = 0.0008$). This constitutes a robust absorbed dose–response relationship. At a patient level, a significant difference was found between patients with complete or partial response (210 Gy; 95% CI, 161–274 Gy; $n = 13$) and patients with progressive disease (116 Gy; 95% CI, 81–165 Gy; $n = 9$) ($P = 0.01$). Patients were subsequently grouped according to their average change in TLG. Patients with an objective response (complete or partial) exhibited a significantly higher overall survival than nonresponding patients (stable or progressive disease) (median, 19 mo vs. 7.5 mo; log-rank, $P = 0.01$). **Conclusion:** These results confirm a significant absorbed dose–response relationship in ^{166}Ho radioembolization. Treatment response is associated with a higher overall survival.

Key Words: radioembolization; holmium; dose–response; dosimetry; dose personalization

J Nucl Med 2020; 61:608–612
DOI: 10.2967/jnumed.119.232751

Radioembolization with ^{90}Y- or ^{166}Ho-microspheres is increasingly used in the treatment of primary and secondary liver cancers (*1*). In this procedure, radioactive microspheres are delivered to hepatic tumors via their nutrient arteries (*2*). The goal of radioembolization is to deliver a tumoricidal absorbed dose to tumors while sparing the healthy liver tissue. Although multiple studies have shown that the likelihood for tumor response critically depends on tumor-absorbed dose, the dosing methods that are predominantly used in clinical practice do not incorporate the patient-specific biodistribution (i.e., locally absorbed doses) (*1,3*).

Treatment with ^{166}Ho radioembolization can be preceded by a scout dose consisting of a small batch (i.e., 250 MBq) of rheologically identical ^{166}Ho-microspheres. Official approval (European Economic Area certification mark) was recently obtained in the European Union (QuiremScout and QuiremSpheres; Quirem Medical B.V.). This scout dose has been shown to predict the absorbed dose to the lungs more accurately than ^{99m}Tc-macroaggregated albumin (*4*). And more recently, the scout dose was shown to have a superior predictive value for the intrahepatic therapy absorbed dose distribution (*5*). These findings support the use of a scout dose to better personalize dose planning (i.e., dosimetry) and patient selection. However, the relationship between tumor-absorbed dose and response likelihood, needed for such a treatment personalization, has not yet been established.

The aim of this exploratory study was to analyze the relationship between tumor-absorbed dose, treatment response, and survival in patients treated with ^{166}Ho radioembolization.

MATERIALS AND METHODS

Patient Selection

Candidates for this study were patients who were treated in the Holmium Embolization Particles for Arterial Radiotherapy I and II studies (HEPAR I and II; NCT01031784 (*6*) and NCT01612325 (*7*)), which were conducted between 2009 and 2015. These studies were in accordance with the Declaration of Helsinki and were approved by the local research ethics committee. Before study entry, all patients provided written informed consent (*6*).

In HEPAR I and II, multimodality imaging with ^{18}F-FDG PET/CT and multiphasic liver CT were acquired during work-up. Preparatory angiography was performed several days before treatment, in which extrahepatic vessels were coil-embolized if necessary, and a scout dose of ^{99m}Tc-macroaggregated albumin (150 MBq, Technescan LyoMAA; Mallinckrodt Medical B.V.) was administered to assess the safety and intrahepatic distribution of subsequent administrations. On the day of treatment, ^{166}Ho-microspheres were administered as a second scout dose (i.e., 250 MBq) in the morning and as a treatment dose in the afternoon, with ^{166}Ho SPECT/CT and MR acquisition after both injections. The total amount of administered activity was adjusted to the targeted liver volume, as measured on

For correspondence or reprints contact: Remco Bastiaannet, University Medical Center Utrecht, Heidelberglaan 100, Utrecht, 3584CX, Netherlands.
E-mail: r.bastiaannet@umcutrecht.nl
*Contributed equally to this work.
Published online Oct. 10, 2019.

CT. In HEPAR II, the aimed absorbed dose was 60 Gy for the treated volume (MIRD monocompartment method) (*7*). HEPAR I was a dose-escalation study in which the aimed absorbed dose was varied between 20 and 80 Gy. Treatment was followed by a posttreatment ^{166}Ho SPECT/CT study and an ^{18}F-FDG PET/CT study at the 3-mo follow-up. None of the included patients received concomitant anticancer therapies.

Included patients for the current study were those who underwent an ^{18}F-FDG PET/CT scan at our hospital at baseline and at the 3-mo follow-up, as well as posttreatment ^{166}Ho SPECT/CT as part of the HEPAR I or II studies.

Absorbed Dose–Response Evaluation

Absorbed dose–response evaluation was performed similarly to what was reported earlier by Van den Hoven et al. (*8*). The tumor outlines were automatically defined by setting a patient-relative threshold for activity concentration on the baseline ^{18}F-FDG PET/CT scan using the ROVER (ABX GmBH) software package (*9*). The threshold was based on the aortic blood-pool activity and defined as 2 times the SUV_{mean} corrected for lean body mass (SUL_{mean}) (*10*). Additionally, a volume restriction of 5 mL or more was used. SUL_{mean} and tumor volume were recorded. Total lesion glycolysis (TLG) was calculated by taking the product of SUL_{mean} and tumor volume. The liver was manually delineated on the accompanying low-dose CT, using ROVER.

The ^{166}Ho-microsphere activity distribution after treatment was estimated with quantitative SPECT/CT reconstructions using a quantitative fast Monte Carlo-based reconstructor (Utrecht Monte-Carlo system), which has been previously validated for ^{166}Ho (*11*).

The PET-based tumor and liver outlines were transferred to the corresponding ^{166}Ho SPECT reconstructions, using a rigid registration of the CT scans of the PET and SPECT acquisitions (*12*). The liver contours served as a mask to focus the registration on the liver region only. The liver and tumor outlines were subsequently dilated with 1 cm, to mitigate errors due to resolution, motion, and local registration errors.

The tumor doses were estimated using the activity in these dilated masks and the mass of the original contour. The parenchymal dose was calculated in the same fashion, after subtracting the dilated tumor masks from the liver mask. The dose was assumed to be fully absorbed within each volume of origin (local deposition model) (*13*). For the 3-mo follow-up scans, the tumors were automatically defined in ROVER. The change in TLG was used to determine the metabolic tumor response. The baseline and follow-up images were assessed side by side to ensure that the same tumors were identified. Merged tumors on follow-up imaging were regarded as a single tumor at baseline. In those cases, a weighted average of the absorbed dose was calculated, correcting for tumor volume. Metabolic tumor response was grouped in categories according to PERCIST (*10*). A complete metabolic response (CR) was

TABLE 1
Baseline Characteristics of the 36 Patients

Characteristic	All patients	Responders	Nonresponders
Sex			
Male	17	6	11
Female	19	6	13
Age (y) at therapy	64 (40–84)	67.5 (44–84)	63 (40–74)
Primary tumor type			
Colorectal carcinoma	21	8	13
Breast carcinoma	4	1	3
Cholangiocarcinoma	4	0	4
Uveal melanoma	4	1	3
Neuroendocrine neoplasm	1	1	0
Pancreas carcinoma	1	0	1
Thymoma	1	1	0
Liver volume (mL)	1,938 (1,155–3,842)		
Metabolic tumor volume (mL)	171 (5−1,993)		
Administered activity (MBq)	6,705 (3,676–12,897)	7,632 (3,763–10,217)	6,705 (3,676–12,897)
Previous treatment			
Locoregional (liver)	8	3	5
Systemic	34	11	23
None	2	1	1
WHO status			
0	29	9	20
1	5	2	3
Unknown	2	1	1
Extrahepatic disease at baseline			
No	26	8	18
Yes	10	4	6

Qualitative data are expressed as numbers; continuous data are expressed as median followed by range in parentheses.

achieved if there was a 100% reduction in TLG, a partial metabolic response (PR) was achieved when there was a decrease of at least 45%, a progressive metabolic response (PD) was characterized by an increase of at least 75%, and stable disease (STBD) was defined as an increase of less than 75% and a decrease of less than 45%. Furthermore, these categories were grouped according to objective response (CR + PR) and nonresponse (STBD + PD).

Statistical Analysis

The relation between tumor-absorbed dose and response was assessed both at the level of individual tumors (local response) and at the patient level, in which case the patients were grouped according to PERCIST based on the average change in TLG of all hepatic tumors. Patient-level analysis was performed both including and excluding tumors that formed after baseline (which were labeled as PD). All other analyses ignored the formation of new lesions at follow-up, as they were not targeted by the treatment. Linear mixed-effect models were used to assess the relation between tumor-absorbed dose and response and to account for correlation of tumors within patients. Dose was used as a dependent variable and was log-transformed to fulfill model assumptions. Nested models were compared using the Akaike Information Criterion. The dose–effect relationship was best explained using a random intercept per patient without random slopes. A geometric mean of the tumor-absorbed dose per response category was estimated. On a patient level, response categories CR and PR were merged in the analysis because of the otherwise too limited numbers per category. To test the hypothesis of an ordered relationship across response categories, a trend test was performed, with response as a continuous variable in the model.

Overall survival was defined as the interval between treatment and death from any cause, with censoring of patients who were still alive at their last known follow-up date. The survival curve was estimated by the Kaplan–Meier method. A log-rank test was used to compare median overall survival between patients with and without a metabolic liver response. Baseline characteristics of these groups, consisting of primary tumor type, sex, age, previous treatments, World Health Organization performance score, presence of extrahepatic disease, number of tumors, and tumor load, were scrutinized for differences that could have biased the survival analysis. Analyses were performed using R statistical software, version 3.4.0. A 2-sided P value of less than 0.05 was considered statistically significant.

RESULTS

Thirty-six patients with a total of 98 tumors were included in this study. Baseline characteristics are listed in Table 1. Eleven patients of the HEPAR I study were excluded because they lacked posttreatment ^{166}Ho SPECT/CT ($n = 4$) or the corresponding low-dose CT scan was not available for the ^{166}Ho SPECT ($n = 7$). Five patients of the HEPAR II study were excluded because they lacked posttreatment ^{166}Ho SPECT/CT ($n = 2$), baseline ^{18}F-FDG PET/CT ($n = 1$), follow-up ^{18}F-FDG PET/CT ($n = 1$), or ^{18}F-FDG uptake in the tumor ($n = 1$).

Three patients from the HEPAR I study were administered an activity corresponding to a uniform absorbed dose of 80 Gy to the target volume; all other patients were administered an activity that corresponded to 60 Gy. The median administered activity was 6,705 MBq, with a range of 3,676–12,897 MBq. Thirty-five patients received whole-liver treatment, and 1 patient received lobar treatment.

Local Response

In total, 98 tumors were delineated. The median number of tumors per patient was 2 (range, 1–9). Median tumor-absorbed dose was 162.1 Gy (range, 16.4–715.7 Gy). Median absorbed dose in the healthy liver tissue was 39.9 Gy (range, 7.2–66.4 Gy).

Metabolic tumor response at the 3-mo follow-up was as follows: CR in 32 tumors, PR in 17 tumors, STBD in 28 tumors, and PD in 21 tumors. The local metabolic response versus absorbed dose is plotted graphically in Figure 1.

The geometric mean tumor-absorbed doses in the response categories at a tumor level were as follows: CR, 232 Gy (95% confidence interval [CI], 178–303 Gy); PR, 168 Gy (95%CI, 122–232 Gy); STBD, 147 Gy (95% CI, 113–191 Gy); and PD, 117 Gy (95% CI, 87–159 Gy). Significant differences between CR and STBD ($P = 0.01$) and between CR and PD ($P = 0.0008$) were found. The P value for trend was 0.0005.

An example of a patient exhibiting CR in several tumors with a good preferential microsphere accumulation in and around the tumors is shown in Figure 2.

Patient-Level Response

There were 2 patients with CR, 11 patients with PR, 14 patients with STBD, and 9 patients with PD. Geometric mean tumor-absorbed doses in the response categories at a patient level were as follows: CR or PR, 210 Gy (95% CI, 161–274 Gy); STBD, 152 Gy (95% CI, 117–198 Gy); and PD, 116 Gy (95% CI, 81–165 Gy). The P value for trend was 0.005.

There was a significant difference in tumor-absorbed dose between patients who showed no response (PD or STBD) and patients from the CR or PR group ($P = 0.008$). Regarding metabolic response at a whole-liver level, considering the development of new tumors as well, there were 2 patients with CR, 10 patients with PR, 7 patients with STBD, and 17 patients with PD. There were 3 patients with new intrahepatic tumors, 2 patients with new extrahepatic tumors, and 5 patients with both new extrahepatic and new intrahepatic tumors.

Survival

Median overall survival was 13.5 mo (range, 2–31 mo; 95% CI, 10–16 mo). Median survival was significantly longer in responders (CR or PR patients) (19 mo; range, 8–31 mo) than in nonresponders (7.5 mo; range, 2–27 mo) (log-rank, $P = 0.01$) (Fig. 3). Baseline characteristics of both groups were explored, but no clearly distinguishable differences were evident (Table 1).

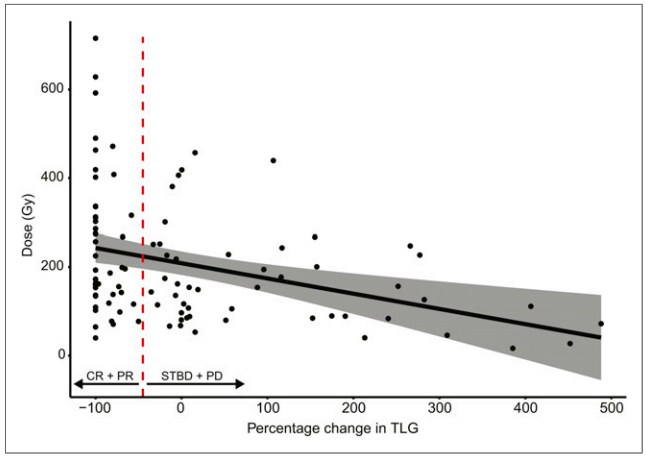

FIGURE 1. Graphical representation of metabolic response vs. absorbed dose of each individual tumor. Decrease in TLG is associated with higher dose. Dashed line indicates cutoff for TLG change, below which metabolic response is defined as CR or PR and above which response is defined as either STBD or PD. Shaded area indicates 95% CI of regression line.

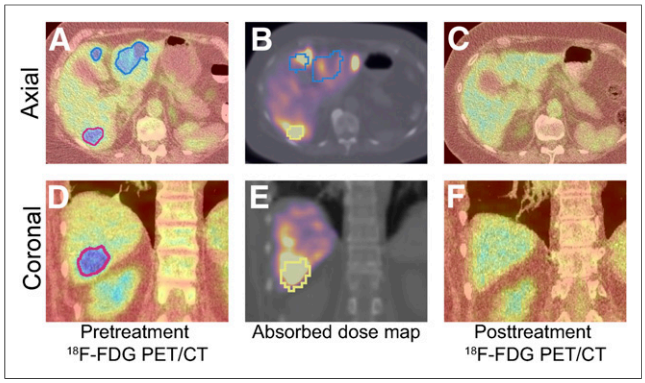

FIGURE 2. Exemplar case in which good spatial correspondence between pretreatment tumor metabolism (A and D) and absorbed dose (average, 120 Gy) (B and E) led to CR (C and F). Tumor outlines are transferred from pretreatment ^{18}F-FDG PET/CT to absorbed dose maps through rigid registration of appurtenant CT scans of SPECT/CT and ^{18}F-FDG PET/CT. In many cases, this registration is imperfect, resulting in slight registration errors, such as is evident in B.

DISCUSSION

This prospective exploratory study was, to our knowledge, the first to show clinical evidence of an absorbed dose–response relationship in patients treated with ^{166}Ho radioembolization. Specifically, a high tumor-absorbed dose was associated with individual tumor and per-patient response, and the occurrence of patient-level objective response was associated with a significantly increased overall survival.

The efficacy of radioembolization with ^{166}Ho-microspheres for inducing anatomic response according to RECIST 1.1 has previously been demonstrated by Prince et al. (*7*). For this study, metabolic metrics were used to measure response. These metrics are more sensitive, often have an earlier onset, and can be more predictive of overall survival (*14*). This was indeed reflected in the higher fraction of patients who were classified as responders at the 3-mo follow-up in the present study (12/36; 33%) than in the study by Prince et al. (5/37; 14%). Furthermore, grouping according to metabolic response resulted in significant differences in overall survival between these groups. This metabolic response was associated with a higher tumor-absorbed dose.

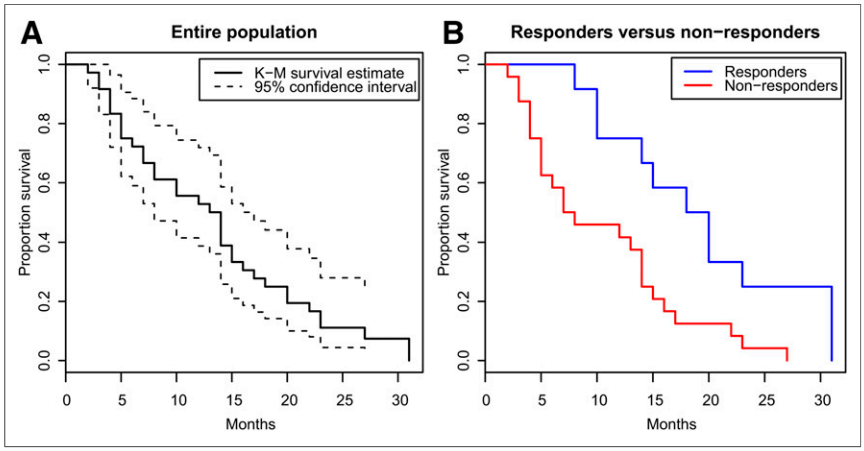

FIGURE 3. (A) Median overall survival for entire study population was 13.5 mo (range, 2–31 mo; 95% CI, 10–16 mo). (B) Median survival was significantly longer in responders (19 mo; range, 8–31 mo) than in nonresponders (7.5 mo; range, 2–27 mo) (log-rank, $P = 0.01$).

van den Hoven et al. conducted a study similar to this one, but with ^{90}Y-resin microspheres in patients with metastatic colorectal cancer (*8*). van den Hoven et al. conservatively estimated that a dose of 40–60 Gy would be needed to achieve a significant tumor response. Willowson et al. found approximately 50 Gy to be sufficient for a metabolic response (*15*), and Levillain et al. found that an average absorbed dose on all tumors higher than 39 Gy was a good predictor of both metabolic response and overall survival (*16*). Flamen et al. found a median of 46 Gy for the metabolic response group (*17,18*). All these studies used resin microspheres in patients with metastatic colorectal cancer. In the current study, the estimated dose needed for a local response was higher (geometric absorbed tumor dose was 232 Gy for CR and 168 Gy for PR). This difference likely reflects differences between the used microspheres and potentially also between the methods used for the actual dose estimation. Furthermore, a direct quantitative comparison with the present study is hampered by heterogeneity in the primary tumor types of the included patient cohort. For a valid pairwise comparison, a more homogeneous patient group is needed.

The semiautomatic method of thresholding the ^{18}F-FDG scans to define tumor volumes, as used in the study, decreased the variance typically induced with manual delineation. By subsequently applying these masks to the corresponding ^{166}Ho dose maps using an automatic registration routine, the current method offered a nonsubjective measure for both dose and response, maximizing reproducibility.

The current study was performed with a limited sample size of patients who had hepatic metastases of different origins. Consequently, there was not enough statistical power to model the differences in ^{18}F-FDG avidity, tumor biology, and radiosensitivity that might exist between the different tumor types. Furthermore, differences in patient positioning and breath-hold policy between PET and SPECT scans, combined with the relatively low resolution and contrast of the low-dose CT portion of the SPECT/CT scan, increased the likelihood of local misregistrations. These effects increased the error in dose estimates in each response group, contributing to a larger spread in each response category and decreasing separability between response groups.

It has been argued that the different radioembolization devices (e.g., resin or glass) result in differences in microdistribution and, consequently, in the absorbed dose needed for tumor response and toxicity (*3*). ^{166}Ho-microspheres are positioned between resin and glass microspheres with respect to the number of injected particles and particle size (*19*). On the basis of these data, we expect the apparent radiosensitivity of ^{166}Ho-microspheres to lie in between as well. However, this expectation will need to be confirmed in a future study in which only patients with the same tumor type are included.

The administered activity in the HEPAR I and II studies was based on the MIRD monocompartment method. In this method, the activity calculation was based on the intended mean absorbed dose to the target liver mass. This method disregards the actual tumor load and the preferential uptake of the microspheres in the tumors, assuming a uniform microsphere distribution in the target volume. The result can be a wide range in actual absorbed tumor doses. However, treatment with ^{166}Ho radioembolization is usually

preceded by administration of a smaller amount of the same microspheres. This scout dose has been shown, relative to ^{99m}Tc-macroaggregated albumin, to enable a more accurate lung shunt fraction estimation (*4*), a safe and improved detection of extrahepatic depositions (*20,21*), and a more accurate pretreatment prediction of the intrahepatic distribution (*5*). These predictive properties may be used to improve patient selection and obtain a more personalized activity prescription by using the pretreatment biodistribution of the scout dose as input to a multicompartment model (e.g., the partition model) (*22*). The prescribed treatment activity can then be maximized such that the absorbed dose in the parenchymal tissue remains below a certain toxicity threshold while maximizing the tumor-absorbed dose (*23*). Subsequent assessment of predicted tumor-absorbed doses can guide patient selection by excluding patients for whom no tumor response is to be expected.

To that end, ^{166}Ho absorbed dose thresholds for specific tumor types need to be established. Future studies will need to focus on a single tumor type, increasing statistical power and enabling the identification of this tumoricidal dose threshold. Similarly, a larger study cohort is needed to establish safe absorbed dose thresholds for the parenchyma. The absorbed dose–response relationship demonstrated in this study shows the feasibility of such an effort and is the first step toward more individualized treatment planning for ^{166}Ho radioembolization.

CONCLUSION

This study found an association between tumor-absorbed dose and local response. Moreover, a patient-level metabolic response was associated with a significant increase in overall survival. Personalized dosimetry has the potential to improve outcome in radioembolization, as has been well established for external-beam radiotherapy.

DISCLOSURE

Marnix Lam is a consultant for BTG International and Terumo. Maarten Smits has served as a speaker for SirTex and Terumo. The Department of Radiology and Nuclear Medicine of the UMC Utrecht receives royalties and research support from Quirem Medical. This work was supported in part by a research grant from Siemens Medical Solutions (Hugo de Jong) and has received funding from the European Research Council (ERC) under the European Union's Horizon 2020 research and innovation program (grant agreement 646734; Hugo de Jong). This work has been partially supported by the ENEN+ project, which received funding from the Euratom Research and Training Work Programme (2016–2017–1 #755576; Remco Bastiaannet). No other potential conflict of interest relevant to this article was reported.

KEY POINTS

QUESTION: What is the relation between absorbed tumor dose and response after radioembolization with ^{166}Ho-microspheres?

PERTINENT FINDINGS: In this prospective study, we were able to show a significant relationship between tumor-absorbed dose and metabolic response (decrease in ^{18}F-FDG uptake). Furthermore, metabolic response was significantly associated with an increase in overall survival by more than a factor 2.

IMPLICATIONS FOR PATIENT CARE: These findings show that personalized dose optimization, which is possible with a ^{166}Ho scout dose, is likely to have a significant impact on tumor response and overall survival.

REFERENCES

1. Reinders MTM, Mees E, Powerski MJ, et al. Radioembolisation in Europe: a survey amongst CIRSE members. *Cardiovasc Intervent Radiol.* 2018;41:1579–1589.
2. Townsend A, Price T, Karapetis C. Selective internal radiation therapy for liver metastases from colorectal cancer. *Cochrane Database Syst Rev.* 2009; CD007045.
3. Bastiaannet R, Kappadath SC, Kunnen B, Braat AJAT, Lam MGEH, de Jong HWAM. The physics of radioembolization. *EJNMMI Phys.* 2018;5:22.
4. Elschot M, Nijsen JFW, Lam MGEH, et al. ^{99m}Tc-MAA overestimates the absorbed dose to the lungs in radioembolization: a quantitative evaluation in patients treated with ^{166}Ho-microspheres. *Eur J Nucl Med Mol Imaging.* 2014; 41:1965–1975.
5. Smits MLJ, Dassen MG, Prince JF, et al. The superior predictive value of ^{166}Ho-scout compared with ^{99m}Tc-macroaggregated albumin prior to ^{166}Ho-microspheres radioembolization in patients with liver metastases. *Eur J Nucl Med Mol Imaging.* August 9, 2019 [Epub ahead of print].
6. Smits MLJ, Nijsen JFW, van den Bosch MAAJ, et al. Holmium-166 radioembolisation in patients with unresectable, chemorefractory liver metastases (HEPAR trial): a phase 1, dose-escalation study. *Lancet Oncol.* 2012;13:1025–1034.
7. Prince JF, van den Bosch MAAJ, Nijsen JFW, et al. Efficacy of radioembolization with 166 Ho-microspheres in salvage patients with liver metastases: a phase 2 study. *J Nucl Med.* 2018;59:582–588.
8. van den Hoven AF, Rosenbaum CENM, Elias SG, et al. Insights into the dose-response relationship of radioembolization with resin ^{90}Y-microspheres: a prospective cohort study in patients with colorectal cancer liver metastases. *J Nucl Med.* 2016;57:1014–1019.
9. ABX advanced biochemical compounds GmbH. ROVER ROI Visualization, Evaluation and Image Registration website. http://www.abx.de/rover/index.php/publishers-details.html. Accessed November 27, 2019.
10. O JH, Wahl RL. PERCIST in perspective. *Nucl Med Mol Imaging.* 2018;52:1–4.
11. Elschot M, Smits MLJ, Nijsen JFW, et al. Quantitative Monte Carlo-based holmium-166 SPECT reconstruction. *Med Phys.* 2013;40:112502.
12. Klein S, Staring M, Murphy K, Viergever MA, Pluim J. Elastix: a toolbox for intensity-based medical image registration. *IEEE Trans Med Imaging.* 2010;29:196–205.
13. Mikell JK, Mahvash A, Siman W, Mourtada F, Kappadath SC. Comparing voxel-based absorbed dosimetry methods in tumors, liver, lung, and at the liver-lung interface for ^{90}Y microsphere selective internal radiation therapy. *EJNMMI Phys.* 2015;2:16.
14. Bastiaannet R, Lodge MA, de Jong HWAM, Lam MGEH. The unique role of fluorodeoxyglucose-PET in radioembolization. *PET Clin.* 2019;14:447–457.
15. Willowson KP, Hayes AR, Chan DLH, et al. Clinical and imaging-based prognostic factors in radioembolisation of liver metastases from colorectal cancer: a retrospective exploratory analysis. *EJNMMI Res.* 2017;7:46.
16. Levillain H, Duran Derijckere I, Marin G, et al. ^{90}Y-PET/CT-based dosimetry after selective internal radiation therapy predicts outcome in patients with liver metastases from colorectal cancer. *EJNMMI Res.* 2018;8:60.
17. Flamen P, Vanderlinden B, Delatte P, et al. Corrigendum: multimodality imaging can predict the metabolic response of unresectable colorectal liver metastases to radioembolization therapy with yttrium-90 labeled resin microspheres (2008 Phys. Med. Biol. 53 6591-603). *Phys Med Biol.* 2014;59:2549–2551.
18. Flamen P, Vanderlinden B, Delatte P, et al. Multimodality imaging can predict the metabolic response of unresectable colorectal liver metastases to radioembolization therapy with yttrium-90 labeled resin microspheres. *Phys Med Biol.* 2008;53:6591–6603.
19. Reinders MTM, Smits MLJ, van Roekel C, Braat AJAT. Holmium-166 microsphere radioembolization of hepatic malignancies. *Semin Nucl Med.* 2019;49: 237–243.
20. Prince JF, van Rooij R, Bol GH, de Jong HWAM, van den Bosch MAAJ, Lam MGEH. Safety of a scout dose preceding hepatic radioembolization with ^{166}Ho microspheres. *J Nucl Med.* 2015;56:817–823.
21. Braat AJAT, Prince JF, van Rooij R, Bruijnen RCG, van den Bosch MAAJ, Lam MGEH. Safety analysis of holmium-166 microsphere scout dose imaging during radioembolisation work-up: a cohort study. *Eur Radiol.* 2018;28: 920–928.
22. Ho S, Lau WY, Leung TWT, Chan M, Johnson PJ, Li AKC. Clinical evaluation of the partition model for estimating radiation doses from yttrium-90 microspheres in the treatment of hepatic cancer. *Eur J Nucl Med.* 1997;24:293–298.
23. Chiesa C, Sjogreen Gleisner K, Flux G, et al. The conflict between treatment optimization and registration of radiopharmaceuticals with fixed activity posology in oncological nuclear medicine therapy. *Eur J Nucl Med Mol Imaging.* 2017;44:1783–1786.